High-temperature properties of oxide-based ceramic matrix composites fabricated with novel mullite fibers

Advanced Materials Research Laboratory, TOSOH Corporation

Yushi NAWATA
Ikuya OHTA
Yo HIRATAKA
Isao YAMASHITA

1. Introduction

Ceramic matrix composites (CMCs) are designed to overcome the brittleness of monolithic ceramic materials while maintaining the advantages of high-temperature stability, excellent mechanical properties, and low density. These materials are thus candidates for potential applications as thermally resistant materials, in aircraft engines, and in power-generating turbines as alternative to conventional nickel super alloys[1–3]. For example, the use of CMCs for aircraft gas-turbine engines improves fuel efficiency and reduces CO_2 reduction. The Leading Edge Aviation Propulsion engine manufactured by CFM International, which employs a high-pressure gas-turbine shroud manufactured using SiC-based CMCs, achieved 15% higher fuel efficiency and 15% lower CO_2 emissions than conventional gas-turbine engine[4].

Figure 1 shows the appearance of monolithic ceramics and CMCs following nail-penetration tests. The monolithic ceramics exhibit fully brittle failure. However, the CMCs maintain their shapes due to their high damage tolerance, which is achieved by deflecting cracks along the weak fiber–matrix interface, uncollected fiber failure, and energy dissipation during fiber pullout[5].

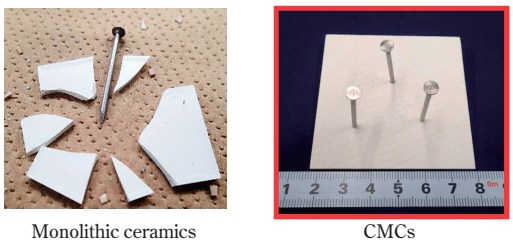

Monolithic ceramics　　CMCs

Fig. 1　Nail penetration test [9]

Oxide-based CMCs (Ox/Ox CMCs), which are composed of oxide fibers and an oxide matrix, have lower cost and better stability against corrosive and oxidative environments than SiC-based CMCs[6]. Thus, Ox/Ox CMCs are promising candidates for high-temperature applications in various oxidizing environments[7].

The thermal stability and high-temperature properties of Ox/Ox CMCs are important factors for their practical applications. We have developed a novel alumina-fiber-based Ox/Ox CMC (TCA-01) and a novel mullite-fiber-based Ox/Ox CMC (TCM-01); both of them exhibit high thermal stability[8,9].

In this technical report, we summarize the high-temperature mechanical properties of the Ox/Ox CMC TCM-01 that we have developed. Our purpose in developing this CMC is to address Sustainable Development Goal 7 (Affordable and Clean Energy) and to contribute to society by providing novel Ox/Ox CMCs.

2. Uniform doping method for oxide fibers

We have developed a novel uniform doping method (UDM)[8,9] to improve the thermal stability of oxide fibers and have used it to produce two Ox/Ox CMCs—TCA-01 and TCM-01—that exhibit high thermal stability. **Figure 2** shows the UDM concept, which is a method of doping oxide fibers (alumina and mullite) with grain-growth inhibitors. This suppresses the grain growth of UDM-treated fibers during thermal exposure. **Figure 3** shows the tensile strengths of the developed Ox/Ox CMCs as processed and after thermal exposure at 1200 ℃ for 1000 h. Neither of the two CMCs that used UDM-treated fibers exhibited a reduction in tensile strength after thermal exposure[8,9].

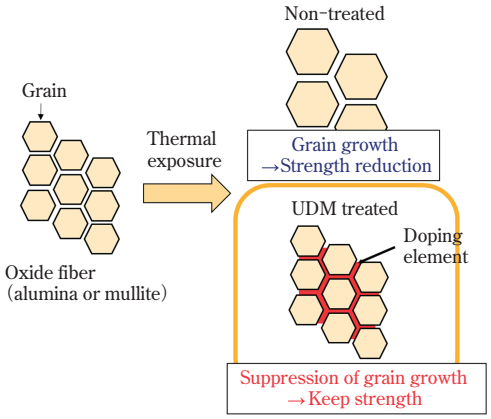

Fig. 2 Concept of uniform doping methods (UDM)

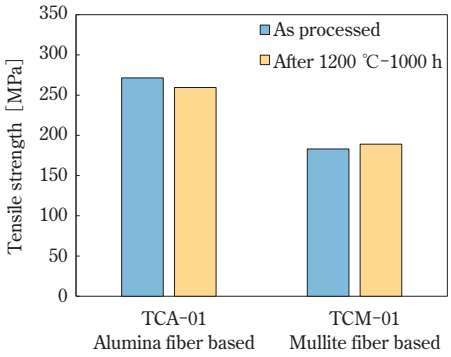

Fig. 3 Tensile strength of developed Ox/Ox as processed and after 1200 ℃ for 1000 h thermal exposure[9)]

3. Mechanical properties of the novel mullite-fiber-based Ox/Ox CMC TCM-01

We developed TCM-01 using UDM-treated mullite fibers and an alumina-based matrix and employing slurry infiltration and a sintering process to fabricate it. **Figure 4** shows optical and scanning electron microscope energy dispersive spectroscopy (SEM–EDS) images of TCM-01. The plate, consisting of five woven layers of this Ox/Ox CMC had a rectangular shape measuring 220 mm by 80 mm with a thickness of 2 mm. The matrix phase filled the spaces between the woven layers of the pile and inside the fiber bundles. The density of TCM-01, measured using Archimedes' method, was 2.62 g/cm^3, and the fiber volume was about 45 volume %.

Table 1 lists the mechanical properties of TCM-01, of a commercially available conventional Ox/Ox CMC using mullite fibers (N720/A ATK-COIC)[10, 13–17], and of a single-crystal nickel-based super alloy for gas-turbine engines (CMSX-4 Cannon-Muskegon)[12, 18]. TCM-01 had better thermal stability than the conventional Ox/Ox

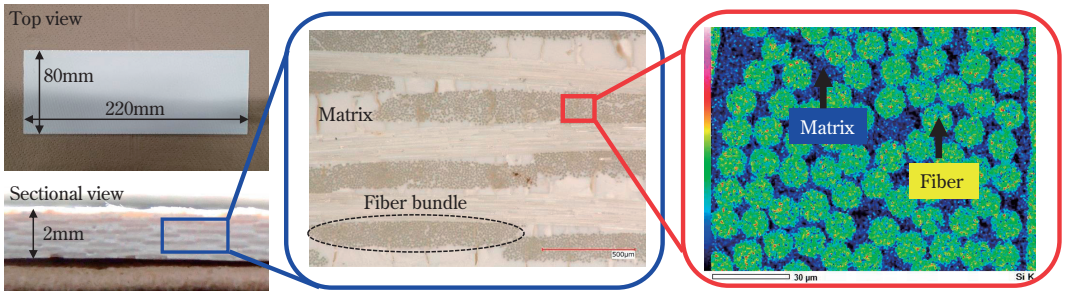

Fig. 4 Optical image and microstructure of TCM-01[9)]

Table 1 Mechanical properties of TCM-01

	Tensile strength at R.T. [MPa]	Retention rate of tensile strength after 1200 ℃ for 1000 h [%]	Tensile strength at 1200 ℃ [MPa]	Creep lifetime at 1200 ℃, 100 MPa [h]
TCM-01	183	103	192	53.8
Conventional Ox/Ox	169[10)]	88	168[13–17),※1]	41[14)]
Sigle crystal Ni-based super alloy	942[12)]	—	172[12)]	13[18),※2]

※1 Average value of tensile strength in the references
※2 At 1200℃, 80 MPa

CMC. We observed no reduction in the tensile strength retention of TCM-01 after being held at 1200 ℃ for 1000 h; in contrast, the tensile strength retention of the conventional Ox/Ox CMC was 88%[10,11].

The tensile properties of TCM-01 at 1200 ℃ were better than those of either the single-crystal nickel-based super alloy or the conventional Ox/Ox CMC. The tensile strength of TCM-01 at 1200 ℃ was 192 MPa, and no significant reduction in tensile strength was observed up to 1250 ℃. For comparison, the tensile strength of a single-crystal nickel-based super alloy at 1200 ℃ was 172 MPa, a significant degradation compared to the results obtained at 24 ℃ (942 MPa)[12]. The tensile strength retention (ratio of tensile strength at 1200 ℃ to room temperature) was 18%. Similarly, the tensile strength of the conventional Ox/Ox CMC at 1200 ℃ was 168 MPa (this value is average value of tensile strength in the references)[13–17].

The creep lifetime of TCM-01 at 1200 ℃ also was better than that of either the single-crystal nickel-based super alloy or the conventional Ox/Ox CMC. The time to rupture of TCM-01 at 1200 ℃ was >100 h at 80 MPa and 53.8 h at 100 MPa. In contrast, the time to rupture the single-crystal nickel-based super alloy at 1200 ℃ was only 13 h at 80 MPa[18], while that of the conventional Ox/Ox CMC at 1200 ℃ was 41.0 h[14] at 100 MPa.

Furthermore, TCM-01 exhibited low thermal conductivity and a high electrical resistivity. The thermal conductivity was 3.3 W/(m/K), which we calculated from the thermal diffusivity evaluated following ASTM E1461, the specific heat, and the density. The electrical resistivity was 1.9×10^{14} Ω cm, which we evaluated following JIS C2141 and JIS C2139, at an applied voltage of 1000 V and a test temperature of 25 ℃.

4. Tensile properties of TCM-01 at high temperature

We performed high-temperature (800–1250 ℃) tensile tests based on the American Society for Testing and Materials (ASTM) C1359 standard in air using a mechanical test machine (MTS Landmark MTS Systems Corporation) and a strain gage (MTS System Corporation). The constant displacement rate was 3.00 mm/min, and we increased the temperature at the rate of 35 ℃/min. We calculated the strain from the crosshead displacement. We used dog-bone-shaped specimens (150 mm long, with an 8-mm-wide gage section). We evaluated the tensile modulus, tensile strength, and proportional limit (0.05% offset). The tensile properties over the range 25–1250 ℃ are listed in **Table 2**. **Figure 5** shows the stress–strain curves over the range 25–1250 ℃, together with the shape and dimensions of the test specimen. **Figure 6** shows the tensile properties of TCM-01 at different temperatures. We observed no significant reduction in the tensile modulus, tensile strength, or proportional limit up to 1250 ℃. Thus, TCM-01 exhibited superior tensile properties at high temperatures up to 1250 ℃.

5. Fatigue properties of TCM-01 at high temperature

We performed high-temperature tension–tension fatigue tests in air using a mechanical test machine (MTS Landmark 370.10 MTS Systems Corporation) and a strain gage (MTS 632.53F-14 MTS System Corporation) based on ASTM C1360. The *R* ratio (the minimum stress divided by the maximum stress) was 0.05 at a frequency of 1 Hz, and the fatigue run-

Table 2　Tensile properties of TCM-01 at high temperature

Test Temperature [℃]	Youg's modulus [GPa]	Proportional limit※1 [MPa]	Tensile strength※2 [MPa]
25	70.6	141	183
800	60.9	125	181
1000	61.0	123	194
1000	61.6	123	194
1100	69.6	127	193
1200	66.2	105	195
1250	57.7	117	180

※1 0.05% offset method, ※2 following ASTM C 1359

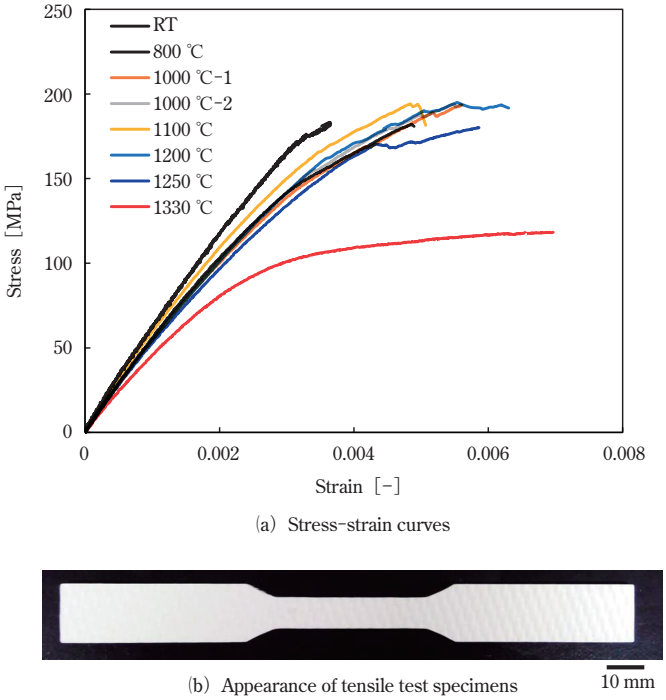

Fig. 5 (a) Stress-strain curves of TCM-01 and (b) appearance of tensile test specimen

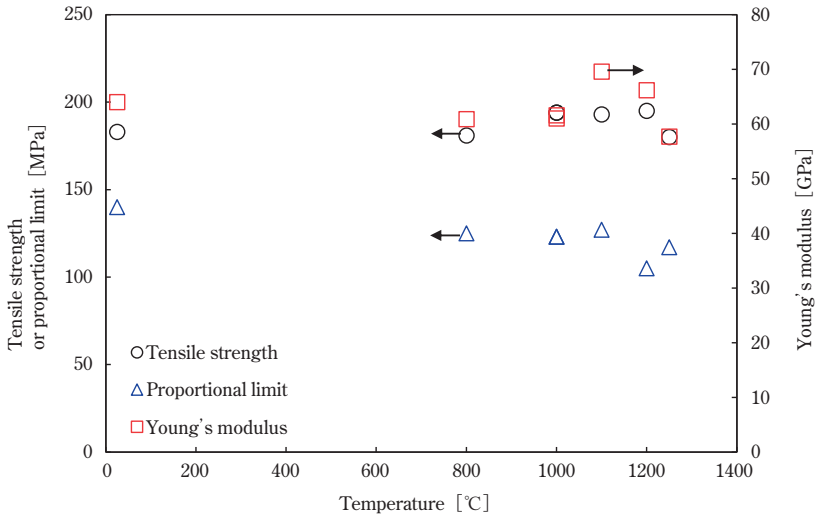

Fig. 6 Tensile properties of TCM-01 at different temperature

out cycle was 10^5. The test temperature was 1200 ℃, and temperature was increased at 35 ℃/min. For this test, we used dog-bone-shaped specimens (200 mm long, with an 8-mm-wide gage section). The test results are listed in **Table 3**, and **Figure 7** shows the typical evolution of a stress–strain hysteresis loop. The maximum stress at run-out at 1200 ℃ was 140 MPa (70% of the ultimate tensile strength at 1200 ℃). Thus, TCM-01 has high fatigue resistance at high temperatures and in environments with high applied stress.

6. Creep properties of TCM-01

We performed creep tests in air using a mechanical test machine (MTS Landmark 370.10 MTS Systems Corporation) and a strain gage (MTS 632.53F-14 MTS System Corporation) based on ASTM C1337. We used the same dog-bone-shaped specimens as for the fatigue test. The test temperatures were 1100, 1150, and 1200 ℃. The stress rate was 15 MPa/s, and the temperature was increased at the rate of 35 ℃/min. The time of creep run-out was 100 h. The test results are listed

Table 3　Results of fatigue tests of TCM-01

Test temperature［℃］	Maximum stress［MPa］	Cycle to failure［−］
1200	100	100,000※
1200	125	100,000※
1200	140	100,000※

※Run-out

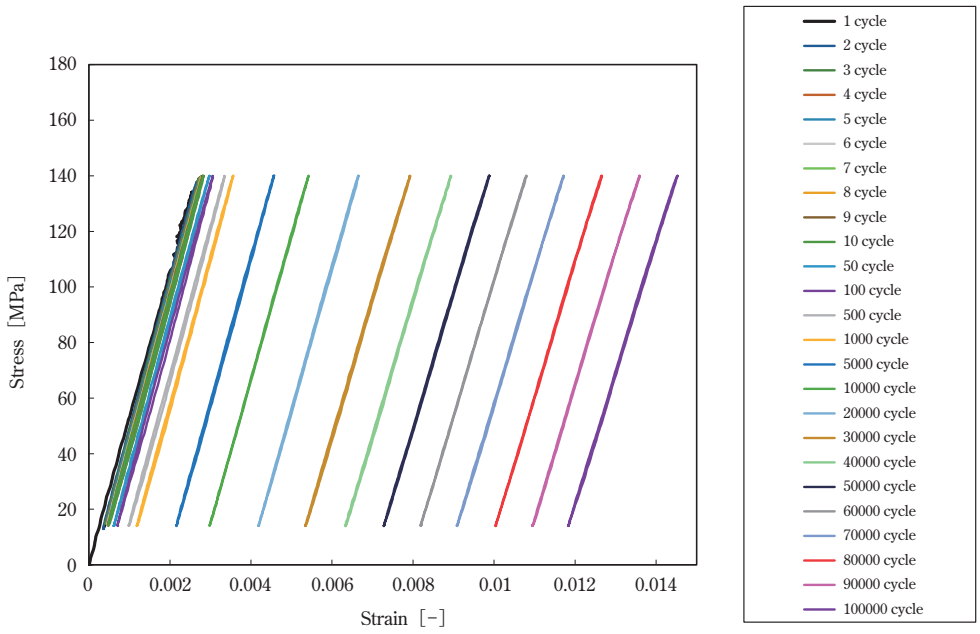

Fig. 7　Typical evolution of a stress-strain hysteresis loop (1200 ℃, 140 MPa)

in **Table 4**, and **Figure 8** shows typical creep strain–time curves. **Figure 9** shows the relationship between the creep stress and the time to rupture. Run-out occurred at a creep stress of 100 MPa at each of the test temperatures 1100 ℃, and 1150 ℃. Therefore, TCM-01 has high creep resistance at high temperatures and in environments with high applied stress.

7.　Thermal shock properties of TCM-01

We performed thermal shock experiments by heating the specimens to different temperatures in a vertical tubular air furnace at a heating rate of 4 ℃/min, and get exposed to air. Air quenching temperature differences (ΔT) is in the range of 0 ℃ to 1175 ℃.We performed the tensile tests using a screw-driven universal mechanical test machine (MTS CriterionTM Model 45 MTS Systems Corporation). The constant displacement rate was 0.50 mm/min. **Figure 10** shows the relative tensile strength of TCM-01 at different ΔT. No remarkable reduction was observed in the relative tensile strength (tensile strength after thermal shock test/tensile strength to that before thermal shock test) of the developed Ox/Ox CMC with ΔT. Thus, these results confirm that the developed Ox/Ox CMC exhibited thermal shock resistance.

Table 4　Results of creep tests of TCM-01

Test temperature［℃］	Stress［MPa］	Time to rupture［h］	Rupture strain［%］
1100	100	100※	—
1150	100	100※	—
1200	80	100※	—
1200	100	53.8	2.98

※Run-out

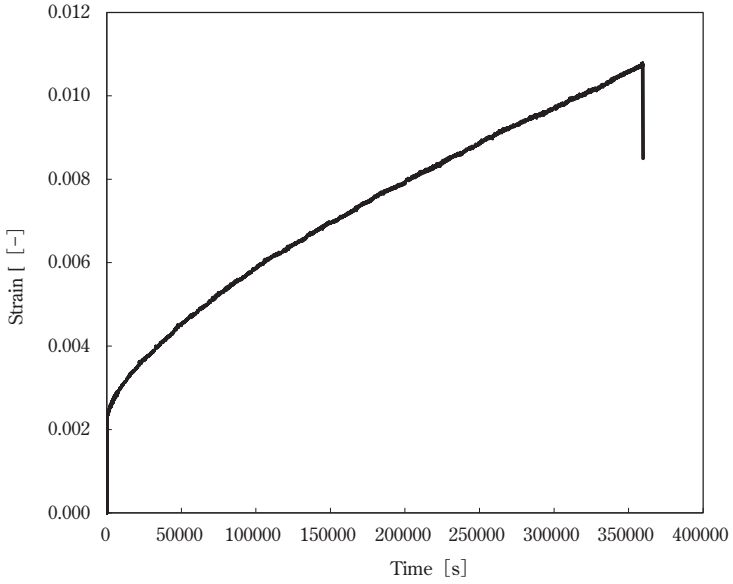

Fig. 8 Typical strain-time relationship (1200 ℃, 80 MPa)

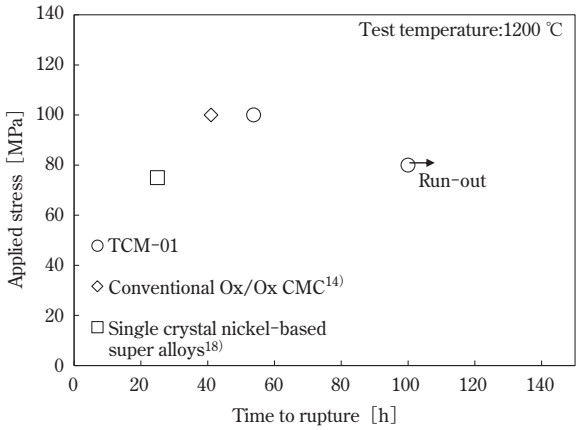

Fig. 9 Creep stress vs time to rupture at 1200 ℃

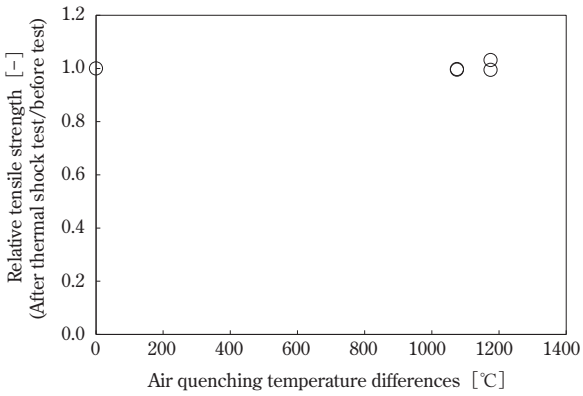

Fig.10 Effect of quenching temperature difference on relative tensile strength of TCM-01

8. Conclusion

In this technical report, we have summarized the high-temperature mechanical properties of TCM-01 using UDM-treated mullite fibers. We found the thermal stability of TCM-01 to be better than that of a conventional Ox/Ox CMC after being held at 1200 ℃ for 1000 h. Additionally, both the tensile strength and the creep lifetime at 1200 ℃ were better than those of either a single-crystal nickel-based super alloy or a conventional Ox/Ox CMC. TCM-01 also exhibited thermal shock resistance. A further increase in the thermal stability can be expected applying UDM and optimizing fabrication process.

We conclude that the Ox/Ox CMC developed in this study can be employed in energy-related materials —particularly thermally resistant materials, aircraft turbines, and power turbines—where long-term thermal stability and superior mechanical properties are required at high temperatures.

Acknowledgments

The authors thank Professors Yutaka Kagawa and Yoshihisa Tanaka at The Center for Ceramics Matrix Composites at Tokyo University of Technology for the use of their evaluation equipment and useful discussions.

References

1）E. Volkmann et al., *Composites Part A*, **68**,19-28 (2015)

2）T. E. Steyer, *International Journal of Applied Ceramic Technology*, **10**, 389-394 (2013)

3）W. Krenkel et al., *Ceramic Matrix Composites, Fiber Reinforced Ceramics and Their Applications*, 327-349 (2014)

4）G. E. Aviation, "The LEAP Engine and MENA Airlines Celebrate 10 Million Hiurs of Lower CO_2 Emissions" <https://www.ge.com/news/reports/the-leap-engine-and-mena-airlines-celebrate-10-million-hours-of-lower-co2-emissions>

5）F. W. Zok, *Journal of the American Ceramic Society*, **89**, 3309-3324 (2009)

6）K. Ramachandran et al., *Journal of the European Ceramic Society*, **42**, 1626-1634 (2022)

7）K. Tushtev et al., *Comprehensive Composite Materials Ⅱ*, (5), 130-157 (2018)

8）I. Yamashita et al., *Proceeding of Ceramic Matrix Composites II: Science and Technology of Materials, Design, Applications, Performance and Integration*, 36 (2022)

9）Y. Nawata et al., *TOSOH Research & Technology Review*, **66**, 85-91 (2022)

10）*Composite Materials Handbook-17-5A*, 79 (2017)

11）S. C. B. Poway, et al., *U. S. Pat*. 20020197465 (2002)

12）A. Sengupta et al., *Journal of Materials Engineering and Performance* **3**, 664-672 (1994)

13）M. B. Ruggles-Wrenn et al., *Composites: Part A*, **37**, 2029-2040 (2006)

14）M. B. Ruggles-Wrenn et al., *Materials Science and Engineering A*, **37**, 101-110 (2008)

15）M. B. Ruggles-Wrenn et al., I*nternational Journal of Fatigue*, **30**, 502-516 (2008)

16）S. G. Steel, *AFIT Scholar Student Graduate Works*, **3**, 132 (2000)

17）L. B. Harlen, *AFIT Scholar Student Graduate Works*, **3**, 112 (2005)

18）J. B. Wahl et al., *Technical report of Cannon-Muskegon* (2018)